POST-SUNSET COOLING BEHAVIOR OF THE LUNAR SURFACE

W. W. MENDELL

Manned Spacecraft Center, NASA, Houston, Texas and Rice University, Houston, Texas, U.S.A.

and

F. J. LOW

Lunar and Planetary Laboratory, Tuscon, Arizona and Rice University, Houston, Texas, U.S.A.

Abstract. Differential infrared flux scans at 22 μm have been made across the nighttime lunar surface over a range of phases before and after new Moon. The differential chopping technique effectively cancels atmospheric emission in the beam path but records the flux difference between adjacent resolution elements on the lunar disk. The scans show that the brightness temperature gradient across the highlands after sunset is much greater than that across the western maria. The large gradients consistently disappear approximately 3.5 days after sunset. The post-sunset enhancement could be due to surface roughness in the highlands or to a significant surface rock population with a mean size of approximately 0.5 m. The effect can be seen in the 10 μm measurements of other investigators, but its global nature was not detected in their limited data sets.

1. Introduction

The discovery of hundreds of 'thermal anomalies' from the infrared mapping of a lunar eclipse by Shorthill and Saari (1969) generated a great deal of interest in the heterogeneity of lunar surface thermal properties. Regional temperature variations related to thermophysical parameters of the surface material are most clearly manifested in the lunar nighttime thermal regime. The cooling time during a lunation is almost fifteen days, and the effects of initial temperature due to topography and albedo should be minimized.

Proper definition of the thermophysical parameters of a lunar region requires monitoring the surface temperature throughout a lunation. This task is a difficult one from the standpoint of astronomical observation. The problem can be solved in the most general sense by mapping the lunar surface in the thermal infrared throughout a lunation. However, a complete nighttime map has yet to be constructed because of low signal levels and observational problems associated with the invisibility of the unilluminated lunar crescent.

A 'lunar cooling curve' is often based on infrared scans across the terminator. Such scans lie approximately parallel to the lunar equator, and points along a scan can be characterized as the temperature versus time of a fictitious lunar region.

Several investigators have measured the post-sunset cooling behavior of the Moon by scanning across the sunset terminator at lunar phases near third quarter (Murray and Wildey, 1964; Shorthill and Saari, 1965; Wildey *et al.*, 1967). In these observations, made at a wavelength of 10 μm, the signal fell to the noise equivalent temperature ($\sim$105 K) of the system before the midnight meridian was reached. The first scans showing the full range of nighttime temperatures were made at 22 μm (Low,

Communication presented at the Conference on Lunar Geophysics, held between October 18–21, 1971, at the Lunar Science Institute in Houston, Texas, U.S.A.

1965). Using this approach, Mendell and Low (1970) filled in the gap in the curve with scans across the sunrise terminator taken after new Moon.

2. Instrumentation and Techniques

A series of lunar infrared scans have been made in right ascension at a variety of phases on either side of new Moon. A spatial resolution element of 27 sec of arc was provided by the 28-in. telescope belonging to the University of Arizona and located in the Catalina Mountains outside Tucson. The Moon's thermal emission was detected with a helium-cooled, doped germanium bolometer (Low, 1961) placed at the Cassegrain focus of the telescope. An interference filter with a spectral bandpass from 17 μm to 25 μm and an effective wavelength of 22 μm sat in front of the detector.

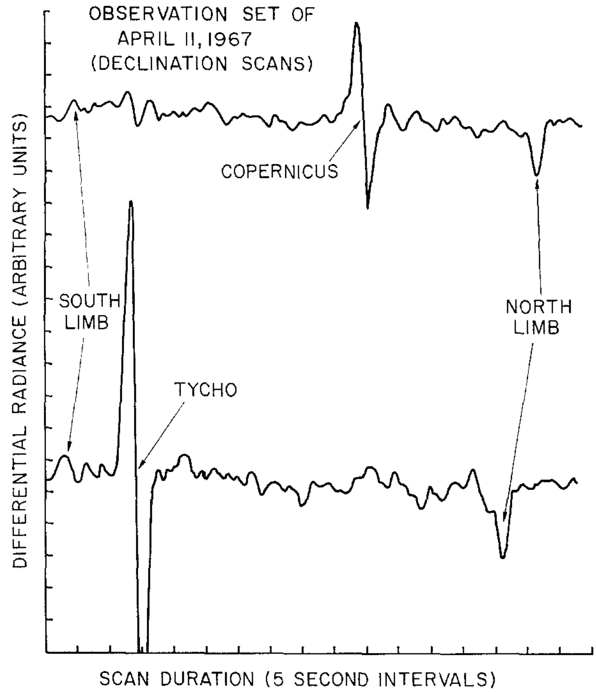

Fig. 1. Declination scans comparing deflections due to Copernicus and Tycho on the nighttime Moon. Copernicus has been unilluminated for 7.8 days and Tycho for 8.5 days.

Scan positions on the Moon were obtained from sightings of features in the illuminated crescent through a boresighted guide telescope.

All scans utilized a differential chopping technique. An oscillating folding mirror reflected energy onto the detector from two adjacent resolution elements in the sky, alternating between them at a rate of 10 Hz. A phase detection circuit separated the signals from the two extreme positions of the mirror and subtracted them. This differenced signal output was integrated over 5 cycles (0.5 s) for each data point. The telescope scanned across the lunar disk while the signal was chopped so that a difference scan of the flux distribution was produced. Details of this observational technique are discussed elsewhere (Mendell, 1971).

Differential chopping effectively cancels atmospheric emission, but the scan baseline must be flat for reconstruction of the flux distribution across the disk. Attempts at reconstruction of the traces resulted in little scan-to-scan correlation. The problem was traced to baseline drifts caused by differential solar heating of the telescope. Very low temperature gradients across the lunar disk added to the uncertainty in the reconstruction. Therefore we are forced to discuss the data in differential form.

Figure 1 illustrates the characteristic signatures of differential lunar scans. In this example both scans were made in declination and lie entirely on the dark side of the Moon. Limb deflections are typical of the sensor response to a step temperature change. As the positive beam and then the negative beam pass over a point source, a characteristic rise and fall of the trace is produced.

3. Discussion of Observations

Figure 2 depicts three right ascension scans. Since they lie approximately perpendicular to the terminator, they follow the lunar 'cooling curve'. Immediately apparent is the contrast between the scans taken prior to new Moon in May, 1968, and the scan taken after new Moon on February 3, 1968. The latter trace has an average value of approximately zero between the cold limb deflection on the left and the morning terminator rise on the right. This characteristic flatness is shared by all scans after new Moon and means that the nighttime temperature gradient over the disk was undetectable.

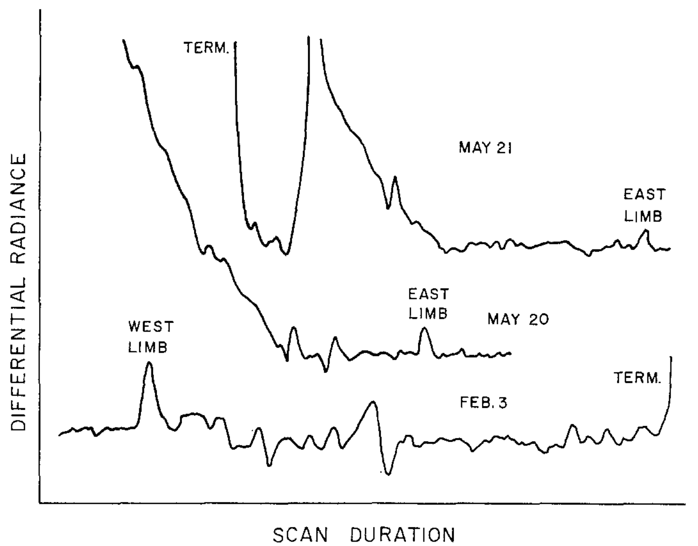

Fig. 2. Typical right ascension differential scans taken before and after new Moon. Scans across the sunset terminator show large scale nonlinear cooling behavior.

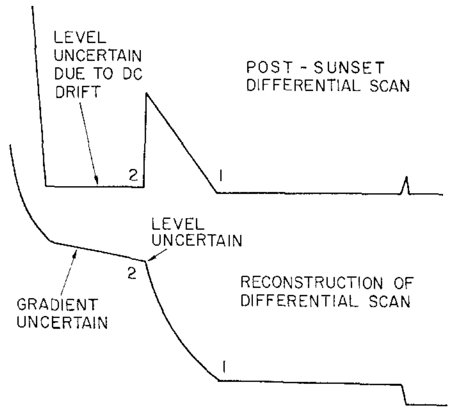

Fig. 3. Simplified version of a post-sunset differential scan illustrating the nature of the reconstructed scan and the associated uncertainties.

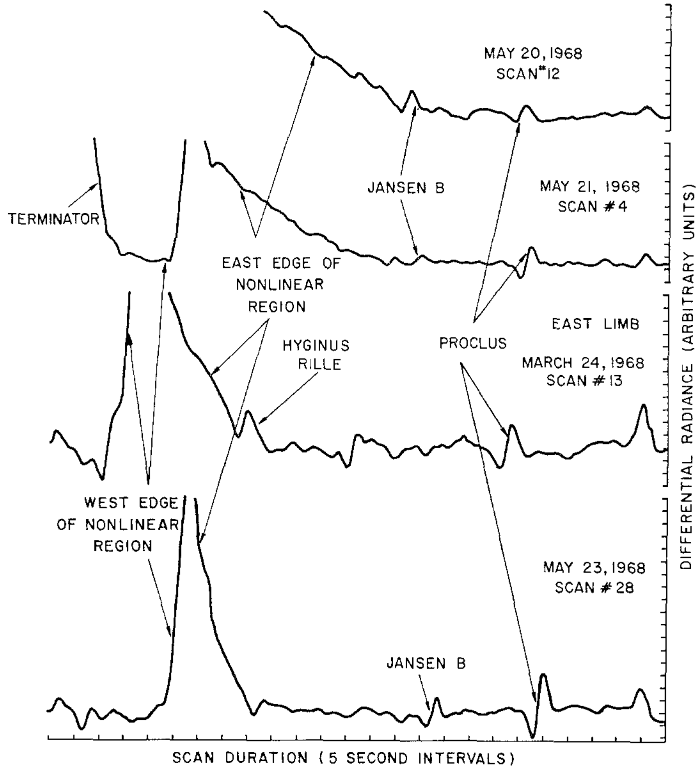

Fig. 4. Scans through the crater Proclus for 4 successive phases of the waning Moon, illustrating the changing structure of the nonlinear cooling region with time. Point-by-point comparisons cannot be made in this figure due to different librations and lunar disk size.

The May 20 scan demonstrates that a detectable temperature gradient exists for some time after sunset. However, on May 21 the evening terminator is moving through a lunar region which is cooling imperceptibly soon after sunset. The last set of a sequence of observations on the waning Moon was taken 4 days before new Moon. At that time, the sunset terminator was still passing through this region.

Figure 3 schematically depicts what is observed and what the true flux distribution should be. Just east of the terminator, the level of the differential scan relative to the scan baseline is uncertain because of the baseline drifts mentioned previously.

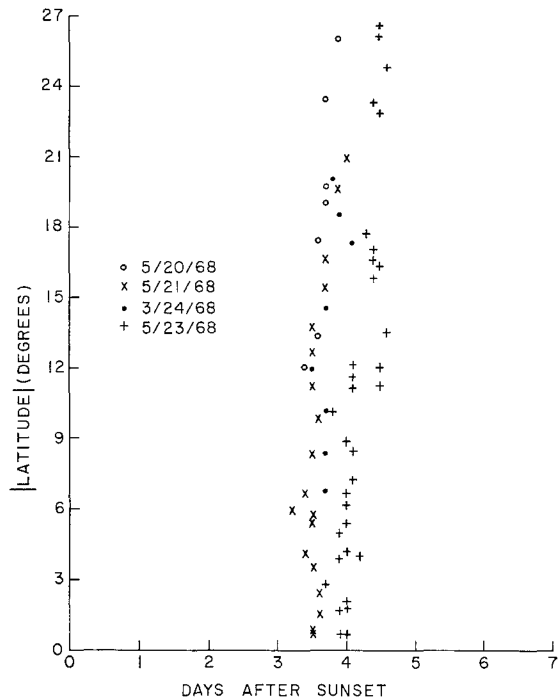

Fig. 5. The location of transition 1 in the lunar cooling curve. The brightness longitude and the absolute value of the latitude are plotted for post-sunset scans during phases of the Moon ranging from 7 days to 4 days prior to new Moon.

Examination of many scans indicates that this level is approximately at the baseline rather than significantly below it. This fact is important because a flat scan is generally caused by the combination of small temperature differences between adjacent resolution elements and a low background temperature. In this case, the lack of a negative excursion to the left of the sharp rise implies that the background temperature is relatively high. Thus the region is cooling very slowly.

The transitions marked 1 and 2 in Figure 3 were studied as a function of phase in order to relate the differential 'cooling curve' to lunar properties. In our observation sets, right ascension scans of the waning Moon exist for the dates May 19–23 and March 24 in 1968. The observations for May 19 and May 22 have a low signal to noise ratio, and cold limb deflections are impossible to identify. The absence of limb deflections precludes the deduction of selenographic positions for features on the scans. Fortunately, the phase of the Moon on March 24 was identical to that on May 22, and the observations cover each phase from 7 days to 4 days before new Moon.

Figure 4 has one scan for each of the four sequential days of observation. Each scan passes through the crater Proclus. The May scans make an angle with the lunar equator of 22°, while the angle for the March scan is 17°. The scans cannot be directly compared point for point because the observing conditions and scan rate vary from

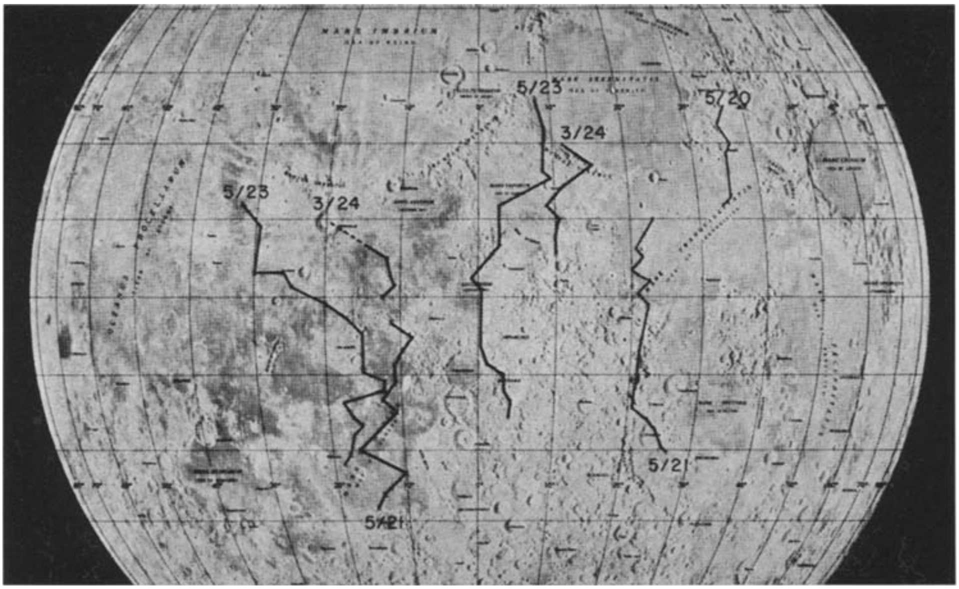

Fig. 6. Available data on the location of transition 1 (eastern longitudes) and 2 (western longitudes) as a function of lunar phase. The observations cover the phases from 7 days to 4 days prior to new Moon.

day to day. Examination of the figure reveals that the two transitions do evolve as a function of phase.

The location of transition #1 in terms of brightness longitude (relative to the terminator) and the absolute value of latitude is plotted in Figure 5 for a number of scans. For any one day the transition falls along a line of constant brightness longitude. There is some tendency for the brightness longitude to be a function of phase, but the effect could easily be due to experimental error. The figure does clearly demonstrate that this transition is a global phenomenon associated with the general cooling curve.

In Figure 6 the location of both transitions is plotted on a lunar map. Transition

#2 seems to be associated with the boundary between the western maria and the central and Copernican highlands. It is definitely less mobile than transition #1, and indeed its apparent movement with phase may be due to difficulties in properly defining the transition on the scans or to changes in the sensitivity of the measurement from set to set. The dotted portion of the locus of #2 for 3/24 means that the exact location is uncertain due to the presence of the large Copernican anomaly.

Since transition #1 is the boundary between regions of detectable and undetectable temperature gradients, it simply may represent the sensitivity limitation of the measurement. The published data from other investigators was searched in order to resolve this point. Figure 7 is reproduced from a previous paper (Mendell and Low, 1970, Figure 5) and shows the best current information on the lunar cooling curve. In each of the three post-sunset data sets, there is a break in slope at about 3.5 days after sunset. The last data point in each of the two earliest scans (Murray and Wildey, 1964; Shorthill and Saari, 1965) falls below the slope which one might extrapolate after the break. Although no error bars are presented with the data, the last point

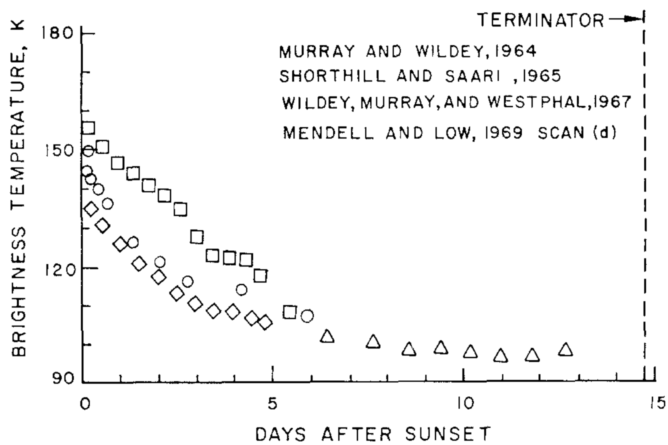

Fig. 7. Measurements of the lunar cooling curve, after Mendell and Low (1970).

should be the noisiest and least reliable. Therefore the idea of a break in the curve followed by a much smaller temperature gradient is not necessarily contradicted. Since all these measurements were made at 10 μm, the temperature dependence of the emitted flux is distinctly different than at 22 μm. The existence of a break in slope of the derived temperature curve at the same point would appear to support the idea that the effect has a lunar rather than instrumental origin.

A search for a published scan, taken at the proper phase and location to see the second transition, has turned up the trace in Figure 8 from Murray and Wildey (1964). Scan VI from their paper passes over Mare Nubium at a phase 4.5 days prior to new Moon. The low cooling rate of the mare is clearly contrasted to the steep slope of the trace in the adjoining highlands.

4. Conclusions

Differential infrared flux scans of the nighttime lunar surface have revealed at least two types of regional cooling behavior. The western maria have a low, undetectable cooling rate soon after sunset. The lunar highlands have a much higher cooling rate for at least 3.5 days after sunset, at which time the cooling rate abruptly becomes undetectable. The data is insufficient to determine the cooling behavior of the eastern maria. After new Moon, the entire nighttime surface cools at a low rate.

It can be inferred from Figure 3 that the highlands begin the lunar night at a

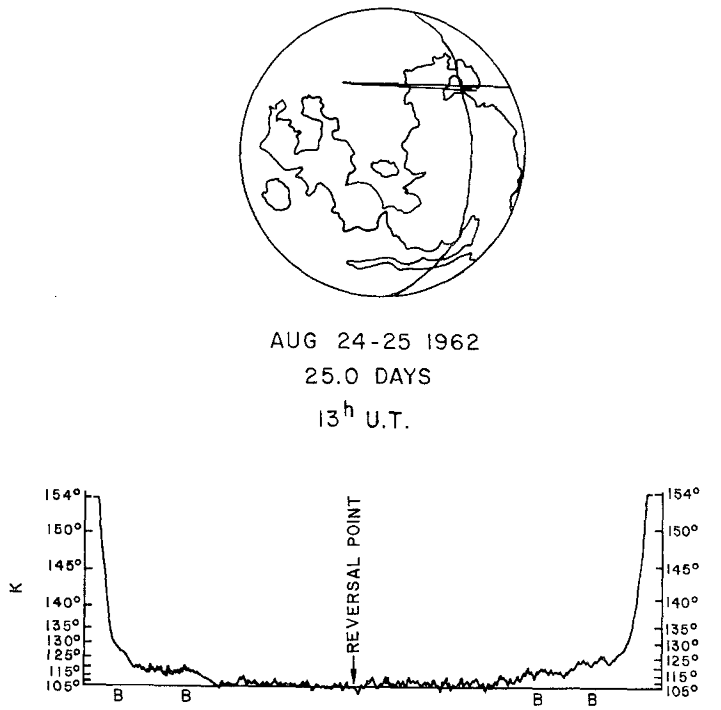

Fig. 8. Post-sunset darkside scan across Mare Nubium from Murray and Wildey (1964).

higher 22 μm brightness temperature than do the western maria. We assume that the mare curve typifies the thermal behavior of a lunar soil, whereas the brightness temperature of the highlands is temporarily enhanced after sunset. We propose two candidates for the enhancement mechanism: the increased surface roughness of the highlands and/or the presence of surface boulders there.

Thermal contour maps of the illuminated Moon (Saari and Shorthill, 1967) have linear cooling patterns in the maria in the lunar afternoon. The highland contours are much more irregular and tend to follow surface morphology. Just prior to sunset the illuminated westward slopes are heated to lunar midday temperatures, while the eastward slopes are prematurely shadowed. The infrared sensor collects all the emitted flux within a resolution element and therefore weights the various temperatures differently. In the temperature range of interest, the detector-filter combination used in this work weights the temperatures according to exp $(-T_0/T)$, where $T_0=654$ K. Areas at higher temperatures are emphasized beyond their actual areal contribution to a resolution element.

We can describe qualitatively the apparent cooling behavior of a rough area whose infrared brightness temperature is T_b due to the presence of a small areal fraction of elevated temperatures. It can be compared to a flat plain whose actual (and infrared) temperature is T_b. At first, the shaded portion will make only a small contribution to the flux from the rough area. The measured cooling behavior is dominated by the small area with elevated temperature, T_1. Consequently the initial cooling rate of the rough area will be a factor of $(T_1/T_b)^4$ greater than the smooth area. As T_1 decreases, the exponential weighting factor of the infrared sensor also decreases, thereby enhancing the apparent cooling rate. If this cooling rate is still decreasing at the time it falls below the detection capability of the differential sensor, the transition will appear to be sharp.

The problem with this explanation may lie in the required time scale. Buhl *et al.* (1968), have studied the phenomenon of enhanced brightness temperatures from cratered surfaces and conclude the net effect of crater geometry is to increase the effective thermal parameter of the material. Thus the area remains enhanced throughout the lunar night. The amount of enhancement depends on the depth to diameter ratio of the craters and the density of cratering. However, the analysis neglects subsurface lateral conduction; and Winter (1969) has shown this restriction leads to significant errors in the post-sunset temperature distribution across the crater. Further calculation can resolve this point.

An alternative explanation of the nonlinear cooling behavior involves the presence of a surface rock distribution. A rock sitting on the lunar surface is warmer than its surrounding at sunset because it receives direct solar illumination even at low sun angles. The size of the rock determines whether it will come into equilibrium with the soil during the night. From data published by Winter (1969), we infer that rocks approximately 50 cm in linear dimension will remain enhanced over the soil background for 3.5 to 4 days after sunset.

Acknowledgements

This work was supported in part by the National Aeronautics and Space Administration under Grant NGR 03-002-110. Special thanks are due Wilbur Griffin who collected the data used in this paper.

References

Buhl, David, Welch, William J., and Rea, Donald G.: 1968, *J. Geophys. Res.* **73**, 7593.
Low, F. J.: 1961, *J. Opt. Soc. Am.* **51**, 1300.
Low, F. J.: 1965, *Astrophys. J.* **142**, 806.

Mendell, W. W. and Low, F. J.: 1970, *J. Geophys. Res.* **75**, 3319.
Mendell, W. W.: 1971, Lunar Differential Flux Scans at 22 μ's, Master's Thesis, Rice University.
Murray, Bruce C. and Wildey, Robert L.: 1964, *Astrophys. J.* **139**, 734.
Saari, J. M. and Shorthill, R. W.: 1967, Isothermal and Isophotic Atlas of the Moon, *NASA Report CR-855*, September, 1967.
Shorthill, Richard W. and Saari, John M.: *Ann. New York Acad. Sci.* **123**, 722.
Shorthill, R. W. and Saari, J. M.: 1969, *Boeing Sci. Res. Lab. Dcmt. D1-82-0778*, January, 1969.
Wildey, Robert L., Murray, Bruce C., and Westphal, James A.: 1967, *J. Geophys. Res.* **72**, 3743.
Winter, Donald F.: 1969, *Boeing Sci. Res. Lab. Dmct. D1-82-0900*, September, 1969.